



HAL
open science

Binuclear Cu(I) and Mn(0) Complexes with a Tridentate Pyridine-NHC-Phosphane Ligand in a μ - κ 2 \hat{C},N -M; κ 1 P-M Coordination Mode

Jérémy Willot, Noël Lugan, Dmitry A. Valyaev

► **To cite this version:**

Jérémy Willot, Noël Lugan, Dmitry A. Valyaev. Binuclear Cu(I) and Mn(0) Complexes with a Tridentate Pyridine-NHC-Phosphane Ligand in a μ - κ 2 \hat{C},N -M; κ 1 P-M Coordination Mode. *European Journal of Inorganic Chemistry*, 2019, 2019 (39-40), pp.4358-4364. 10.1002/ejic.201900628 . hal-02361486

HAL Id: hal-02361486

<https://hal.science/hal-02361486>

Submitted on 6 Nov 2020

HAL is a multi-disciplinary open access archive for the deposit and dissemination of scientific research documents, whether they are published or not. The documents may come from teaching and research institutions in France or abroad, or from public or private research centers.

L'archive ouverte pluridisciplinaire **HAL**, est destinée au dépôt et à la diffusion de documents scientifiques de niveau recherche, publiés ou non, émanant des établissements d'enseignement et de recherche français ou étrangers, des laboratoires publics ou privés.

Binuclear Cu(I) and Mn(0) Complexes with a Tridentate Pyridine-NHC-Phosphine Ligand in a μ - $\kappa^2\hat{C},N$ -M; κ^1P -M Coordination Mode

Jérémy Willot,^[a] Noël Lugan^{*[a]} and Dmitry A. Valyaev^{*[a]}

Abstract: The reaction of a non-symmetrical pyridine-NHC-phosphine (NCP) ligand – generated *in situ* upon the deprotonation of the corresponding imidazolium salt – with equimolar amount of [Cu(NCMe)₄](BF₄) or Mn₂(CO)₁₀ leads to the formation of bimetallic complexes [Cu₂(NCP)₂(NCMe)](BF₄)₂ and [Mn₂(CO)₇(NCP)], respectively, in which the tridentate ligand exhibits an unusual μ - $\kappa^2\hat{C},N$ -M; κ^1P -M coordination mode. According to NMR spectroscopy and mass spectrometry, the binuclear copper complex is in equilibrium in MeCN solution with two mononuclear species, namely [Cu($\kappa^2\hat{C},P$ -NCP)](BF₄) and [Cu(κ^3-N,\hat{C},P -NCP)(NCMe)](BF₄).

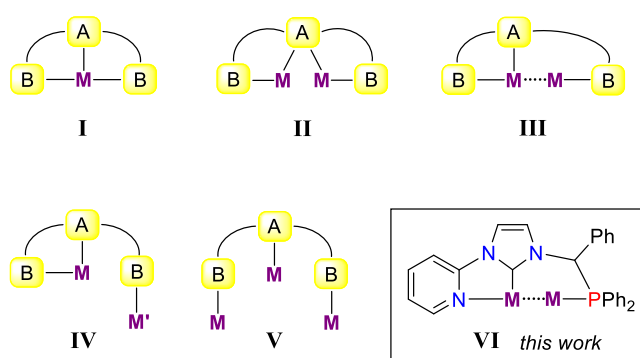
Introduction

Pincer-type ligands are very popular scaffolds in transition metal chemistry and homogeneous catalysis.^[1] While the formation of mononuclear complexes with meridional κ^3 -M coordination (Scheme 1, (I)) reinforced by two five- and/or six-membered chelating cycles clearly makes a reputation for this class of ligands, several alternative tridentate coordination modes are known as well (Scheme 1, (II-V)). In particular, the central aryl,^[2] amide,^[3] phosphide,^[4] pyridine,^[5] phosphole^[6] or *N*-heterocyclic carbene (NHC)^[7] unit can occupy a μ^2 -bridging position in bimetallic complexes II, while the two peripheral donor groups are symmetrically bound to both metal atoms. Alternatively, various pincer-type ligands can adopt a κ^2 -M; κ^1 -M' coordination mode to form binuclear compounds III, in which metal atoms are linked by a covalent bond or a metallophilic interaction,^[8-12] as well as mono-^[13] or polymeric^[11b,11d,14] complexes IV lacking of any metal-metal bonding. Finally, in the trimetallic species V each donor moiety of the triphos,^[15] P-NHC-P,^[16] or NHC-Py-NHC^[17] ligands can be coordinated to the corresponding metal atom without any chelating stabilization.

Though the formation of compounds III with terpyridine,^[8] pybox-,^[9] triphos-,^[10] and PNP-type^[11] ligands is quite well documented, such derivatives bearing other pincer-like architectures still remain scarce.^[12] Taking into account remarkable application of some compounds II-V in photophysics^[3b,15f,16b,17a] or homogeneous catalysis,^[8b,9b,9d] the design of multimetallic systems based on new tridentate ligands remains highly topical. We report herein, the synthesis,

spectroscopic and structural characterization of bimetallic transition metal complexes VI (Scheme 1) bearing non-symmetric pyridine-NHC-phosphine ligand exhibiting a μ - $\kappa^2\hat{C},N$ -M; κ^1P -M coordination mode.

Scheme 1. Diverse coordination modes of tridentate ligands in transition metal complexes

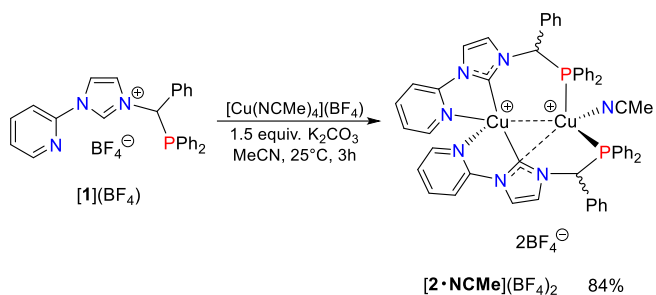


Results and Discussion

Being aware that the imidazolium salt [1](BF₄) (Scheme 2) can be used as precursor for the corresponding NHC-core pincer ligand NCP in rhodium and nickel chemistry,^[18] we decided to expand the scope of this ligand to copper taking into account some literature precedents for the successful preparation of mononuclear κ^3P,N,P -Cu(I) species.^[19] We have initially observed that the reactions of free NCP ligand 1, obtained upon deprotonation of [1](BF₄) using KHMDS, with [Cu(NCMe)₄](BF₄) under various reaction conditions led to the formation of intricate mixtures of products. By contrast, the addition of K₂CO₃ as a weak base to an equimolar mixture of [1](BF₄) and [Cu(NCMe)₄](BF₄) in acetonitrile at room temperature cleanly afforded complex [2•NCMe](BF₄)₂ isolated in 84% yield as yellow-green crystals (Scheme 2). The X-ray diffraction study on single crystals obtained from the concentrated MeCN solution revealed, however, the formation of a binuclear structure (Figure 1a), in which two unsymmetrical NCP ligands adopt a head-to-head arrangement. The recrystallization of [2•NCMe](BF₄)₂ from a CH₂Cl₂/Et₂O mixture afforded the complex [2](BF₄)₂ (Figure 1b) showing a similar arrangement of the ligands but now lacking the

[a] Dr. J. Willot, Dr. N. Lugan, Dr. D. A. Valyaev
LCC-CNRS, Université de Toulouse, CNRS, UPS, Toulouse,
France
205 route de Narbonne, 31077 Toulouse Cedex 4, France
E-mail: noel.lugan@lcc-toulouse.fr, dmitry.valyaev@lcc-toulouse.fr
<https://www.lcc-toulouse.fr/article388.html>

Supporting information for this article is given via a link at the end of the document.



Scheme 2. Synthesis of binuclear Cu(I) complex $[2 \cdot NCMe](BF_4)_2$

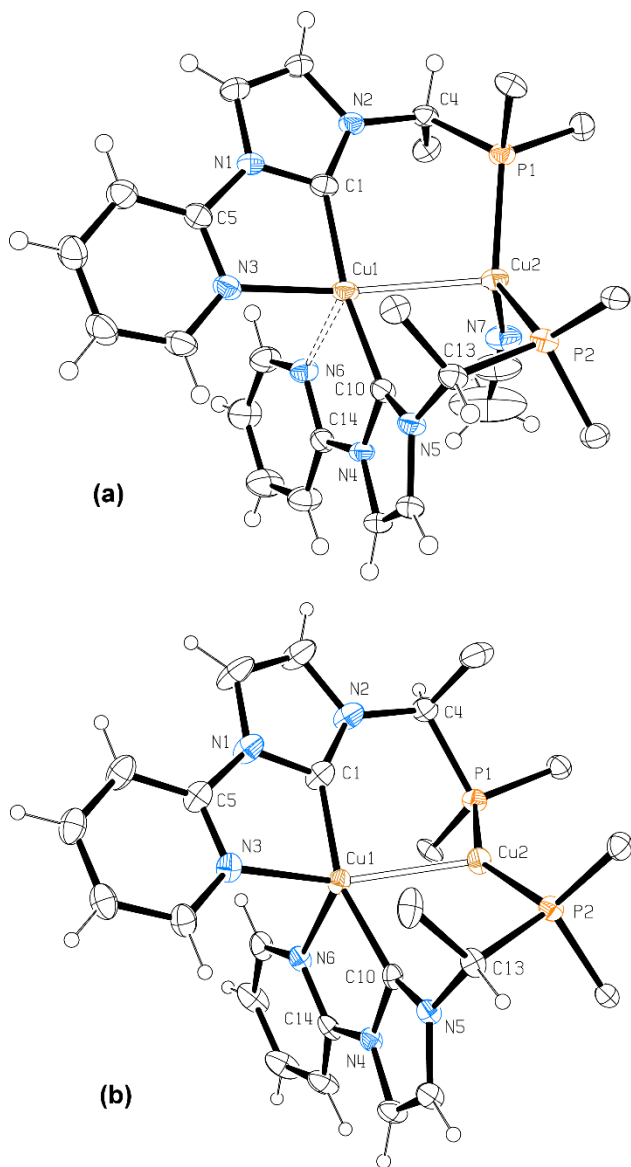


Figure 1. Molecular geometry of complexes $[Cu_2(N\dot{C}P)_2(NCMe)](BF_4)_2$ $[2 \cdot NCMe](BF_4)_2$ (a) and $[Cu_2(N\dot{C}P)_2](BF_4)_2$ $[2](BF_4)_2$ (b). Ellipsoids are given at 30% probability level, BF_4^- anions and solvate CH_2Cl_2 for $[2](BF_4)_2$ are omitted. For the reason of clarity, only C_{ipso} atoms of phenyl groups are shown.

acetonitrile ligand. The formation of the latter isomer can be tentatively explained by a combination of well-known lability of monodentate nitrogen ligands in Cu(I) complexes in solution and stabilization of the another form containing a half of solvate CH_2Cl_2 molecule in the crystal cell. The most pertinent metrical data for these copper complexes are given in the Table 1.

Both complexes belong to the structural type **III** (Scheme 1), in which pyridine-NHC and phosphine moieties are coordinated to the Cu1 and Cu2 atoms exhibiting a typical metallophilic interaction.^[20] To the best of our knowledge, only one similar structure with non-symmetrical tridentate scaffold is known in literature, namely the Cu(I) complex based on oxazoline-pyridine-phosphaalcene ligand.^[12f] The Cu1...Cu2 distance in complex $[2](BF_4)_2$ is ca. 0.2 Å shorter than the one found in the related binuclear Cu(I) complex bearing bidentate NHC-phosphine ligands in a bridging head-to-head arrangement.^[21] As compared to $[2](BF_4)_2$, the coordination sphere of Cu2 atom in $[2 \cdot NCMe](BF_4)_2$, being completed by an acetonitrile ligand, induces, in particular, the elongation of Cu–P bonds by 0.04–0.07 Å and a significant decrease of P1–Cu2–P2 angle (124.79(4)° vs. 149.67(8)° for $[2](BF_4)_2$ and $[2 \cdot NCMe](BF_4)_2$, respectively). In contrast, the Cu1–NHC bond distances in both complexes remain the same within the experimental error and only a small change of the linear C1–Cu1–C2 arrangement can be noticed. Interestingly, one of the NHC moieties shows a semi-bridging character the Cu2...C10 distances of 2.531(6) and 2.799(3) Å in $[2](BF_4)_2$ and $[2 \cdot NCMe](BF_4)_2$, respectively, being below the sum of van der Waals radii of these atoms (3.1 Å). These distances are however longer than those observed in examples of Cu(I) complexes clearly exhibiting semi-bridging NHCs (2.285(9)–2.310(3) Å).^[17b,22] It can also be mentioned that the Cu1–N6 distances related to the pyridine moiety being connected to the semi-bridging NHC is systematically longer than the Cu1–N3 distances in the other ligand. Finally, the configuration of the chiral centers at C4 and C13 was found to be different for $[2](BF_4)_2$ (*RS/SR*) and $[2 \cdot NCMe](BF_4)_2$ (*SS/RR*) demonstrating that some structural reorganization is possible in solution (*vide infra*).

Table 1. Selected bond distances (Å) and angles (°) for Cu(I) the complexes $[2](BF_4)_2$ (left column) and $[2 \cdot NCMe](BF_4)_2$ (right column)

$[Cu_2(N\dot{C}P)_2](BF_4)_2$			$[Cu_2(N\dot{C}P)_2(NCMe)](BF_4)_2$		
Cu1–C1 1.930(7)	Cu1–C10 1.933(7)	Cu2...C10 2.531(6)	Cu1–C1 1.934(3)	Cu1–C10 1.915(3)	Cu2...C10 2.799(3)
Cu1–N3 2.098(6)	Cu1–N6 2.148(6)	Cu1...Cu2 2.4179(11)	Cu1–N3 2.135(2)	Cu1–N6 2.349(3)	Cu1...Cu2 2.6179(5)
–	Cu2–P1 2.2105(19)	Cu2–P2 2.2109(19)	Cu2–N7 2.012(3)	Cu2–P1 2.2566(8)	Cu2–P2 2.2865(11)
C1–Cu1–C10 161.1(3)	P1–Cu2–P2 149.67(8)		C1–Cu1–C10 168.62(13)	P1–Cu2–P2 124.79(4)	
C1–Cu1–N3 82.3(3)	C10–Cu1–N6 81.0(2)		C1–Cu1–N3 81.43(10)	C10–Cu1–N6 77.06(11)	

The analysis of the NMR spectroscopy data for complexes **[2](BF₄)₂** and **[2-NCMe](BF₄)₂** appeared not to be trivial. At room temperature, the ³¹P NMR spectra of both complexes in CD₃CN display a major signal at δ_P 6.8 ppm and two broad resonances of equal intensity at δ_P 12.2, and -1.1 ppm (Figure 2, top). Upon cooling to -40 °C, the signals of the minor species become broad doublets at δ_P 12.4 and -2.4 ppm with a J_{PP} coupling constant of 82.0 Hz (Figure 2, bottom). While ¹H spectrum at 25 °C was not very informative due to line broadening, at -40 °C, the key signals of the major complex could be successfully attributed. In particular, the characteristic resonance of *CHPh* bridge between NHC and phosphine moiety appears at δ_H 6.73 ppm as a virtual triplet with J_{PH} of 4.2 Hz. On the other hand, the signals of *CHPh* and carbene carbon atoms in ¹³C{¹H} spectrum recorded at low temperature, also appeared as virtual triplets at δ_C 63.9 (J_{PC} = 14.2 Hz) and 183.2 (J_{PC} = 15.6 Hz) ppm, respectively.

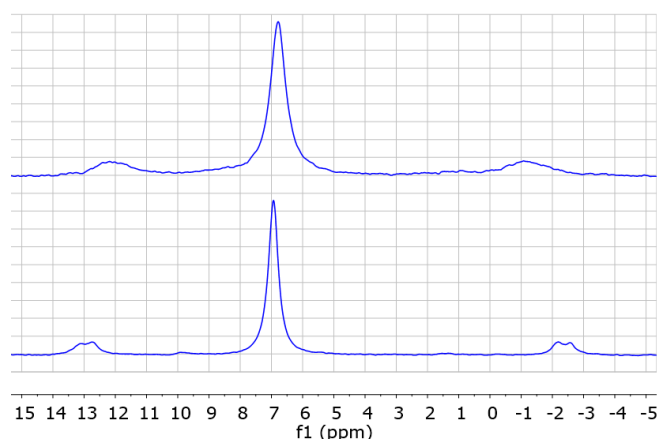


Figure 2. ³¹P{¹H} spectra of complex **[Cu₂(NĈP)₂](BF₄)₂ at 298K (top) and 233K (bottom) (202.5 MHz, CD₃CN).**

In order to get more information about the dynamic processes occurring in solution for the Cu(I) complex, we have carried out ³¹P-³¹P 2D-EXSY experiments at different temperatures (Figure 3). Despite a modest signal/noise ratio due to low amount of minor complex in solution and signal broadening, at 30°C, we have unambiguously observed the presence of cross-peaks evidencing the interconversion between two observed complexes (Figure 3a). At a slightly lower temperature of 10 °C, this process become undetectable while further cooling to -10°C evidences another exchange process now involving the minor compound only.

The analysis of the sample by ESI mass-spectrometry in MeCN solution reveals the presence of the molecular peak of the cationic part of the parent bimetallic compound **[Cu₂(NĈP)₂]²⁺** (*m/z* 482.5) as well as two mononuclear complexes of the composition **[Cu(NĈP)₂]⁺** (*m/z* 901.4) and **[Cu(NĈP)(NCMe)]⁺** (*m/z* 522.9) (Figure S7). Additionally, the peaks of **[Cu(NCMe)₂]⁺** (*m/z* 145.0) and imidazolium salt **[1]⁺** (*m/z* 420.4) are observed.

Based on the NMR and mass-spectrometry data we propose that the bimetallic complex **[2](BF₄)₂** actually constitutes the minor species observed in the ³¹P NMR spectra, the two inequivalent phosphorus nuclei exhibiting a typical ²J_{PP} coupling constant of

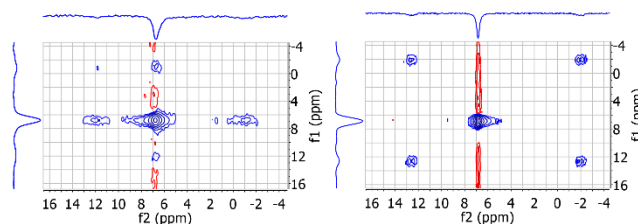
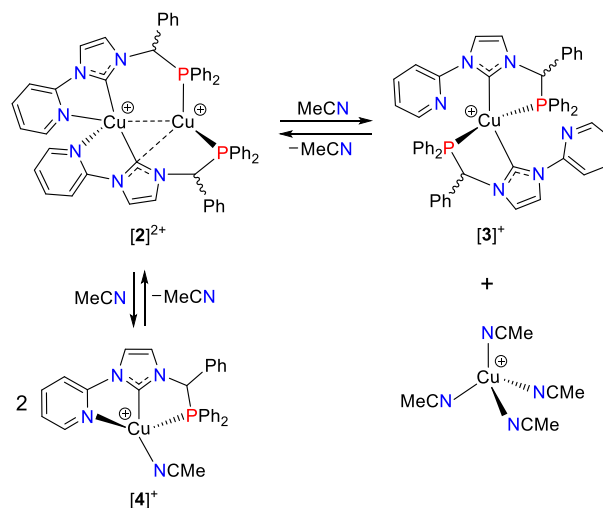


Figure 3. ³¹P-³¹P 2D EXSY spectra (202.5 MHz, CD₃CN) of complex **[Cu₂(NĈP)₂](BF₄)₂ at 303K (left) and 233K (right).**

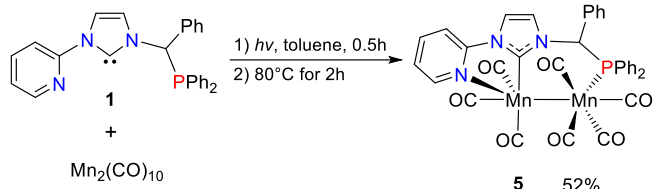
82.0 Hz. This compound would undergo a reversible dissociation in solution to form the mononuclear complex **[3](BF₄)** bearing two NĈP ligands in a κ²C,P coordination mode (Scheme 3). The structure of this complex showing a [distorted] tetrahedral arrangement of the ligands around the metal atom can be inferred from the equivalence of the coordinated phosphorus nuclei (singlet at δ_P 6.8 ppm in the ³¹P NMR spectra) and virtual triplets observed for *CHPh* and carbene atoms the ¹H and ¹³C spectra, clearly showing that in the major species the two NHC and the two phosphine moieties are coordinated to the same metal atom. Additionally, due to the relatively labile character of Cu(I)-NHC bonding well documented in literature,^[23] the **[2](BF₄)₂** species could also reversibly form two molecules of complex **[4](BF₄)** containing a MeCN ligand and a tridentate NĈP ligand presumably in κ³N,C,P coordination mode (Scheme 3). Though we have no distinct NMR signature for this product, it could be the actual intermediate in the automerization process of **[2](BF₄)₂** observed by ³¹P-³¹P 2D-EXSY at -10°C (Figure 3, right).



Scheme 3. Proposed dynamic processes taking place in the case of binuclear Cu(I) complex **[2](BF₄)₂** in acetonitrile solution

Considering that complexes **II-V** (Scheme 1) mainly dealt with coinage metals, we were curious to know whether the present unsymmetrical NĈP ligand would allow similar coordination mode to be observed with other transition metals. In a continuation of our interest to manganese NHC complexes,^[24]

we thus decided to evaluate the reactivity of the free NCP ligand **1** with the Mn(0) precursor $\text{Mn}_2(\text{CO})_{10}$. Under UV irradiation, the reaction led to the formation of the binuclear complex $[\text{Mn}_2(\text{CO})_7(\text{NCP})]$ (**5**) isolated in 52% yield after purification by column chromatography (Scheme 4). This result differs from thermal reaction of $\text{Mn}_2(\text{CO})_{10}$ with two equivalents of PNP ligand precursor in the presence of hexamethyldisiloxane leading to the isolation of pincer complex $[(\kappa^3P,N,P-(i\text{Pr})_2\text{PCH}_2\text{CH}_2)_2\text{N}]\text{Mn}(\text{CO})_2$ in 67% yield.^[25]



Scheme 4. Synthesis of binuclear Mn(0) complex **5** with bridging NCP ligand

Compound **5** belongs to the relatively underdeveloped Mn(0) NHC complexes family.^[26] Solution IR spectrum of **5** shows seven ν_{CO} bands in a 2022–1873 cm^{-1} domain. In ^{13}C spectrum, the signal of the carbenic atom, observed as a doublet at δ_{C} 215.2 ppm with a $^2J_{\text{PC}}$ coupling of 8.0 Hz, is located in the same region as previously observed for $\text{Mn}_2(\text{CO})_9(\text{NHC})$ parent complexes.^[26b]

The exact structure of **5** was inferred from an X-ray diffraction analysis (Figure 4). As for the Cu(I) complexes **[2](BF₄)₂** and **[2·NCMe](BF₄)₂**, the tridentate NCP ligand is coordinated in μ - $\kappa^2\hat{\text{C}},N\text{-M};\kappa^1P\text{-M}$ fashion. The Mn–Mn bond length (2.9584(3) Å) is slightly longer than in the $\text{Mn}_2(\text{CO})_{10}$ precursor (2.9078(2) Å)^[27] and compares well with the one found in the binuclear complex $\text{Mn}_2(\text{CO})_9(\text{IMes})$ (2.9576(4) Å)^[26b] bearing a NHC ligand in *trans* position relative to the metal-metal bond. The Mn–NHC bond distance in **5** (1.9700(17) Å) is shorter than the one found in

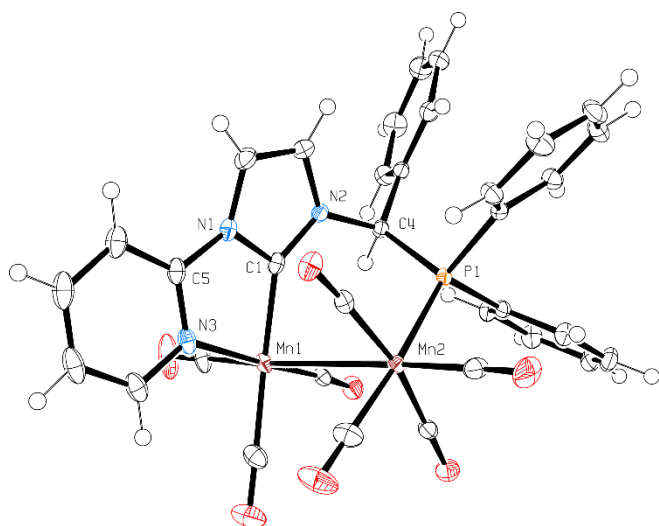


Figure 4. Molecular geometry of complex $[\text{Mn}_2(\text{CO})_7(\text{NCP})]$ **5** (30% probability ellipsoids). Selected bond distances (Å) and angles (°): Mn1–Mn2 2.9584(3), Mn1–C1 1.9700(17), Mn1–N3 2.0860(14); Mn2–P1 2.3272(5), C1–Mn1–N3 77.44(6).

$\text{Mn}_2(\text{CO})_9(\text{IMes})$ (2.0339(18) Å) and belongs to the shortest known for any Mn–NHC complexes, being comparable only with the values observed in half-sandwich Mn(I) NHC complex tethered with a Cp ligand (1.964(2) and 1.963(2) Å).^[24b]

Conclusions

We have shown that the tridentate pyridine-NHC-phosphine ligand is flexible enough to form in good yield bimetallic species in which NHC-pyridine and phosphine donors bridge two proximate metal atoms connected either by a metallophilic interaction or by metal-metal covalent bond. These results demonstrate the utility of non-symmetrical pincer-type architectures for the design of unusual bi- and polymetallic compounds with possibly interesting photochemical or catalytic properties. The studies in this direction is actually in progress in our group.

Experimental Section

General considerations. All manipulations were carried out using Schlenk techniques under an atmosphere of dry nitrogen. Dry and oxygen-free organic solvents (THF, Et₂O, CH₂Cl₂, toluene, pentane) were obtained using LabSolv (Innovative Technology) solvent purification system. Acetonitrile was dried over P₂O₅ and distilled under argon prior to use. Hexane and toluene used for column chromatography purification were deoxygenated by nitrogen bubbling during 15–20 min. Imidazolium salt **[1](BF₄)¹⁸** and **[Cu(NCMe)₄(BF₄)²⁸** were prepared according to previously described procedures. All other reagent grade chemicals purchased from commercial sources were used as received. Synthesis of complex **5** was carried out using a home-made external 10 W light source based on 395–405 nm LEDs. Chromatographic purification of the compounds was performed on silica (0.060–0.200 mm, 60 Å) obtained from Acros Organics flushed with nitrogen just before use. Solution IR spectra were recorded in 0.1 mm CaF₂ cells using a Perkin Elmer Frontier FT-IR spectrometer and given in cm^{-1} with relative intensity in parentheses. ¹H, ³¹P, and ¹³C NMR spectra were obtained on Bruker Avance 400, Avance III HD 400 and Avance 500 spectrometers and referenced to the residual signals of deuterated solvent (¹H and ¹³C) and to 85% H₃PO₄ (³¹P external standard). When necessary the additional information on the carbon signals attribution was obtained using ¹³C{¹H,³¹P} and ¹H–¹³C HMQC experiments. Elemental analysis was carried out in LCC-CNRS (Toulouse, France) using Perkin Elmer 2400 series II.

Synthesis of complex [2·NCMe](BF₄)₂. To a solution of **[1]BF₄·0.4THF** (107 mg, 0.2 mmol) in MeCN (10 mL) solid **[Cu(NCMe)₄(BF₄)** (63 mg, 0.2 mmol) was added at room temperature and the solution was stirred for 1 h. Then K₂CO₃ (41 mg, 0.3 mmol) was added and the resulting mixture was stirred for two additional hours and then filtered through Celite. The solution was concentrated to ca. 2–3 mL and ether (10 mL) was added dropwise with a stirring to induce the precipitation of the target complex. The supernatant was removed by decantation and the precipitate was dried under vacuum to afford **[2·NCMe](BF₄)₂** (99 mg, 84%) as yellow microcrystalline powder. Single crystals of **[2·NCMe](BF₄)₂** suitable for X-ray diffraction experiment were obtained from concentrated solution of complex in acetonitrile at room temperature. The dissolution of the sample of **[2·NCMe](BF₄)₂** in CH₂Cl₂ and vapor diffusion of ether allowed to prepare the single crystals of other form of this complex **[2](BF₄)₂** lacking the coordinated MeCN ligand. Due to the occurrence of two dynamic

processes in solution, the amount of [2](BF₄)₂ was relatively low and it was reliably detected only by ³¹P NMR spectroscopy. The major component in CD₃CN solution [Cu(κ²N, C-NCP)₂](BF₄) was fully characterized by multinuclear NMR spectroscopy.

[2-NCMe](BF₄)₂: ³¹P{¹H} NMR (202.5 MHz, CD₃CN, 25 °C): δ 12.2 (br s), -1.1 ppm (br s). ³¹P{¹H} NMR (202.5 MHz, CD₃CN, -40 °C): δ 12.9 (d, ²J_{PP} = 81.2 Hz), -2.4 ppm (d, ²J_{PP} = 83.8 Hz). Anal. Calcd. for C₅₆H₄₇B₂Cu₂F₈N₇P₂ (M = 1180.7) C, 56.97; H, 4.01; N, 8.30. Found: C, 56.92; H, 4.21; N, 8.53. We were unable to obtain acceptable microanalysis data for copper complex [2](BF₄)₂, probably because of a variable amount dichloromethane trapped in the solid samples.

[3](BF₄)₂: ¹H NMR (500.3 MHz, CD₃CN, 25 °C): δ 8.05 (br s, 1H, Py), 8.03 (br s, 1H, Ph), 7.86 (br d, ³J_{HH} = 7.2 Hz, 1H, Py), 7.61 (s, 1H, CH_{Im-4,5}), 7.55–7.47 (m, 2H, Ph), 7.45–7.23 (m, 9H, Ph + Py), 7.21–7.10 (m, 3H, Ph + CH_{Im-4,5}), 6.93 (br t, ³J_{HH} = 6.1 Hz, 1H, Ph), 6.89–6.76 (m, 2H, Py), 6.68 ppm (br s, 1H, CHPh). ¹H NMR (500.3 MHz, CD₃CN, -40 °C): δ 8.05 (d, ³J_{HH} = 14.1 Hz, 1H, Py), 8.04 (s, 1H, Ph), 7.88 (d, ³J_{HH} = 8.3 Hz, 1H, Py), 7.58 (s, 1H, CH_{Im-4,5}), 7.51 (d, ³J_{HH} = 14.1 Hz, 2H, Ph), 7.45–7.27 (m, 9H, Ph + Py), 7.22–7.15 (m, 3H, Ph + CH_{Im-4,5}), 6.87 (t, ³J_{HH} = 7.3 Hz, 1H, Ph), 6.78 (t, ³J_{HH} = 7.6 Hz, 2H, Py), 6.73 ppm (vt, J_{PH} = 4.1 Hz, 1H, CHPh); ³¹P{¹H} NMR (202.5 MHz, CD₃CN, 25 °C): δ 6.8 ppm (s). ³¹P{¹H} NMR (202.5 MHz, CD₃CN, -40 °C): δ 6.9 ppm (s). ¹³C{¹H} NMR (125.8 MHz, CD₃CN, -40 °C): δ 182.3 (vt, J_{CP} = 15.6 Hz, Cu–CN₂), 149.4 (s, C_{ipso} Py), 148.6 (s, CH_{Py}), 141.6 (s, CH_{Py}), 135.8 (br s, CH_{Ph}), 134.7 (vt, J_{CP} = 7.7 Hz, CH_{PPH₂}), 134.1 (d overlapped with another d, ¹J_{CP} = 18.2 Hz, C_{ipso} PPH₂), 134.0 (d overlapped with another d, ¹J_{CP} = 15.6 Hz, C_{ipso} PPH₂), 132.1 (s, C_{ipso} Ph), 132.8 (vt, J_{CP} = 7.4 Hz, CH_{PPH₂}), 131.8 (s, CH_{Ph}), 131.4 (s, CH_{Ph}), 129.8 (br d, J_{CP} = 4.2 Hz, CH_{PPH₂}), 129.6 (br vt, J_{CP} = 4.5 Hz, CH_{PPH₂}), 129.3 (s, CH_{Ph}), 128.7 (s, CH_{Py}), 126.5 (s, CH_{Im-4,5}), 124.0 (s, CH_{Im-4,5}), 112.7 (s, CH_{Py}), 63.9 ppm (vt, J_{CP} = 14.2 Hz, PC(H)Ph).

Synthesis of complex (5). To a suspension of [1]BF₄•0.4THF (80 mg, 0.15 mmol) in toluene (10 mL) a 0.5M solution of KHMDS in toluene (330 μL, 0.165 mmol) was added dropwise at room temperature. The reaction mixture was sonicated for 5 min and stirred for additional 5 min. To the resulting orange solution of free NHC 1 solid Mn₂(CO)₁₀ was added and the solution was irradiated with UV light under vigorous stirring with IR monitoring. IR data showed gradual disappearance of starting Mn₂(CO)₁₀ (ν_{CO} 2046 (s), 2011 (vs), 1982 cm⁻¹ (m br)) and the formation of new species with very complex IR spectrum. The irradiation was continued until the characteristic ν_{CO} bands of the product at 1965 (vs) and 1948 cm⁻¹ (vs) ceased to increase (ca. 30-40 min). Then Schlenk tube was removed from the reactor and heated in the oil bath at 80°C for 2 h leading to additional increase of the ν_{CO} bands of the target product 5. The resulting deep-orange solution was cooled to room temperature, filtered through Celite and evaporated under vacuum. The residue was purified by column chromatography on silica (7×1 cm). Elution with hexane/toluene 1:1 mixture afforded first yellow band containing traces of unreacted Mn₂(CO)₁₀ followed by yellow band containing a small amount of unidentified manganese carbonyl complexes (discarded). The product 5 was eluted with pure toluene as large orange band. The eluate was evaporated under vacuum and the orange residue was dissolved in the 1:1 mixture of THF with degassed heptane (20-25 mL), filtered through Celite and concentrated to ca. 10 mL to induce the crystallization of the product finished at -20°C overnight. The supernatant was removed by decantation and the precipitate was washed with hexane (5 mL) and dried under vacuum to afford complex 5 (62 mg, 52%) as red-orange crystals containing according to ¹H NMR and microanalysis data one molecule of THF solvate. Single crystals of 5 suitable for X-ray diffraction were obtained by vapor diffusion of hexane to the solution of complex in ether at room temperature.

⁵: ¹H NMR (400.1 MHz, CD₂Cl₂, 25 °C): δ 9.05 (br d, ³J_{HH} = 5.7 Hz, 1H, Py), 7.90 (td, ³J_{HH} = 8.3 Hz, J_{HH} = 1.2 Hz, 1H, Py), 7.76–7.70 (m, 3H, Ph), 7.68 (d, ³J_{HH} = 8.3 Hz, 1H, Py), 7.50 (td, ³J_{HH} = 7.4 Hz, J_{HH} = 1.1 Hz, 1H, Py), 7.44–7.39 (m, 3H, Ph + CH_{Im-4,5}), 7.37–7.30 (m, 3H, Ph), 7.24 (t, ³J_{HH} = 7.7 Hz, 2H, Ph), 7.19–7.09 (m, 3H, Ph), 6.91 (d, ³J_{HH} = 2.3 Hz, 1H, CH_{Im-4,5}), 6.79 (d, ³J_{HH} = 7.7 Hz, 2H, Ph), 5.93 (d, ²J_{PH} = 3.0 Hz, 1H, CHPh), 3.68 (m, 4H, OCH₂CH₂ THF), 1.82 ppm (m, 4H, OCH₂CH₂ THF). ³¹P{¹H} NMR (162.0 MHz, CD₂Cl₂, 25 °C): δ 126.0 ppm (br s). ¹³C{¹H} NMR (100.6 MHz, CD₂Cl₂, 25 °C): δ 229.9 (s, Mn–CO), 229.3 (br s, Mn–CO), 228.3 (s, Mn–CO), 226.0 (br s, Mn–CO), 225.2 (br s, Mn–CO), 223.4 (br s, Mn–CO), 221.9 (s, Mn–CO), 215.2 (d, ²J_{CP} = 8.0 Hz, Mn–CN₂), 154.0 (s, CH_{Py}), 150.8 (s, C_{ipso} Py), 137.6 (s, CH_{Py}), 135.1 (d, ¹J_{CP} = 28.5 Hz, C_{ipso} PPH₂), 134.5 (d, ¹J_{CP} = 35.3 Hz, C_{ipso} PPH₂), 134.4 (d, J_{CP} = 11.1 Hz, CH_{PPH₂}), 132.9 (d, J_{CP} = 8.1 Hz, CH_{PPH₂}), 132.9 (s, C_{ipso} Ph), 132.7 (d, J_{CP} = 3.3 Hz, CH_{Ph}), 131.5 (d, J_{CP} = 1.8 Hz, CH_{Ph}), 130.6 (d, J_{CP} = 1.0 Hz, CH_{Ph}), 129.9 (s, CH_{Ph}), 129.2 (s, CH_{PPH₂}), 128.9 (d, J_{CP} = 9.1 Hz, CH_{PPH₂}), 128.8 (d, J_{CP} = 8.3 Hz, CH_{PPH₂}), 123.0 (d, ³J_{CP} = 2.0 Hz, CH_{Im-4,5}), 119.4 (s, CH_{Py}), 116.0 (d, ⁴J_{CP} = 2.2 Hz, CH_{Im-4,5}), 111.8 (s, CH_{Py}), 69.2 (d, ¹J_{CP} = 3.1 Hz, PC(H)Ph), 68.3 (s, OCH₂CH₂ THF), 26.2 (s, OCH₂CH₂ THF). IR (toluene): ν_{CO} 2022 (vs), 1965 (vs), 1948 (vs), 1920 (s), 1905 (s), 1898 (s), 1873 cm⁻¹ (m). Anal. Calcd. for C₃₄H₂₂N₃PMn₂O₇•THF (M = 797.5) C, 57.23; H, 3.79; N, 5.27. Found: C, 57.21; H, 3.42; N, 4.98.

X-ray diffraction studies. The single-crystal X-ray diffraction data collection was carried out on a Bruker D8/APEX II/Incoatec Mo IμS Microsource diffractometer ([2-NCMe](BF₄)₂, [2](BF₄)₂) and on a Nonius Mach 3/APEX II/sealed Mo X-ray tube diffractometer (5). All calculations were performed on a PC compatible computer using the WinGX system.^[29] The structures were solved using the SIR92 program^[30] and refined by a full-matrix least-squares technique on F² with anisotropic displacement parameters for all non-hydrogen atoms using the SHELXTL program suite.^[31] Atomic scattering factors were taken from the usual tabulations. Anomalous dispersion terms for the Mn and Cu were included in Fc. The hydrogen atoms were set in idealized positions (RCH₃, C–H = 0.98 Å, U_{iso}(H) = 1.5U_{eq}(C); C(sp²)–H = 0.95 Å; U_{iso}(H) = 1.2U_{eq}(C)) and their positions refined as “riding” atoms. One of the BF₄⁻ anions in complex [2-NCMe](BF₄)₂ was disordered over two positions with 1:1 ratio. The hydrogen atoms were set in idealized positions, as described above. After completing the initial structure solution for complexes [2-NCMe](BF₄)₂, it was found that 14% of the total cell volume was filled with disordered solvent molecules, which could not be precisely modeled in terms of discrete molecules. The disordered solvent contribution was then subtracted from the observed data using the SQUEEZE procedure.^[32] CCDC 1919547-1919549 contain the supplementary crystallographic data for the structures unveiled in this paper. These data can be obtained free of charge from the Cambridge Crystallographic Data Centre via www.ccdc.cam.ac.uk/data_request/cif.

Acknowledgments

We thank the Centre National de la Recherche Scientifique (CNRS) for general support of this project. J.W. is grateful to French MENESR for a PhD fellowship.

Keywords: Tridentate ligands • N-Heterocyclic Carbene • Copper • Manganese • X-ray diffraction

- [1] a) *Pincer and pincer-type complexes: applications in organic synthesis and catalysis*, (Eds.: K. J. Szabó, O. F. Wendt), Wiley-VCH, Weinheim, **2014**; b) G. Gunanathan, D. Milstein, *Chem. Rev.* **2014**, *114*,

- 12024–12087; c) L. Alig, M. Fritz, S. Schneider, *Chem. Rev.* **2019**, *119*, 2681–2751.
- [2] a) A. Pape, M. Lutz, G. Müller, *Angew. Chem. Int. Ed.* **1994**, *33*, 2281–2284; b) J. J. Adams, N. Arulsamy, D. M. Roddick, *Organometallics* **2012**, *31*, 1439–1447.
- [3] a) S. B. Harkins, J. C. Peters, *J. Am. Chem. Soc.* **2004**, *126*, 2885–2893; b) S. B. Harkins, J. C. Peters, *J. Am. Chem. Soc.* **2005**, *127*, 2030–2031; c) A. R. Fout, F. Basuli, H. Fan, J. Tomaszewski, J. C. Huffman, M.-H. Baik, D. J. Mendiola, *Angew. Chem. Int. Ed.* **2006**, *45*, 3291–3295.
- [4] N. P. Mankad, E. Rivard, S. B. Harkins, J. C. Peters, *J. Am. Chem. Soc.* **2005**, *127*, 16032–16033.
- [5] Selected examples: a) E. C. Constable, A. J. Edwards, M. J. Hannon, P. R. Raithby, *Chem. Commun.* **1994**, 1991–1992; b) M. Al-Anber, B. Walfort, S. Vatsadze, H. Lang, *Inorg. Chem. Commun.* **2004**, *7*, 799–802; c) Effendy, F. Marchetti, C. Pettinari, R. Pettinari, B. W. Skelton, A. H. White, *Inorg. Chim. Acta* **2007**, *360*, 1414–1423; d) B. Liu, X. Ma, F. Wu, W. Chen, *Dalton Trans.* **2015**, *44*, 1836–1844; e) C. M. A. Farrow, G. R. Akien, N. R. Halcovitch, J. A. Platts, M. P. Coogan, *Dalton Trans.* **2018**, *47*, 3906–3912.
- [6] B. Nohra, E. Rodriguez-Sanz, C. Lescop, R. Réau, *Chem. Eur. J.* **2008**, *14*, 3391–3403.
- [7] S. Gischig, A. Togni, *Organometallics* **2005**, *24*, 203–205.
- [8] Selected recent examples: a) M. J. Hannon, C. L. Painting, E. A. Plummer, L. J. Childs, N. W. Alcock, *Chem. Eur. J.* **2002**, *8*, 2225–2238; b) Y. Cui, C. He, *J. Am. Chem. Soc.* **2003**, *125*, 16202–16203; c) C.-T. Yeung, H.-L. Yeung, C.-S. Tsang, W.-Y. Wong, H.-L. Kwong, *Chem. Commun.* **2007**, *48*, 5203–5205; d) Xiao-Ping Zhou, Shi-Hong Lin, Dan Li, Ye-Gao Yin, *CrystEngComm* **2009**, *11*, 1899–1903; e) M. Gil-Moles, M. Concepcion Gimeno, J. M. Lopez-de-Luzuriaga, M. Monge, M. Elena Olmos, D. Pascual, *Inorg. Chem.* **2017**, *56*, 9281–9290; f) C. L. Mak, B. C. Bostick, N. M. Yassin, M. G. Campbell, *Inorg. Chem.* **2018**, *57*, 5720–5722.
- [9] a) J. Diez, M. P. Gamasa, M. Panera, *Inorg. Chem.* **2006**, *45*, 10043–10045; b) M. Panera, J. Diez, I. Merino, E. Rubio, M. P. Gamasa, *Inorg. Chem.* **2009**, *48*, 11147–11160; c) M. Panera, J. Diez, I. Merino, E. Rubio, M. P. Gamasa, *Eur. J. Inorg. Chem.* **2011**, 393–404; d) G. M. Borrajo-Calleja, Eire de Julian, E. Bayon, J. Diez, E. Lastra, I. Merino, M. Pilar Gamasa, *Inorg. Chem.* **2016**, *55*, 8794–8807.
- [10] Selected examples: a) D. L. DuBois, A. Miedaner, R. C. Haltiwanger, *J. Am. Chem. Soc.* **1991**, *113*, 8753–8764; b) R. D. Hart, B. W. Skelton, A. H. White, *Aust. J. Chem.* **1991**, *44*, 919–925; c) C.-T. Lee, S.-F. Chiang, C.-T. Chen, J.-D. Chen, C.-D. Hsiao, *Inorg. Chem.* **1996**, *35*, 2930–2936; d) C.-T. Lee, W.-K. Yang, J.-D. Chen, L.-S. Liou, J.-C. Wang, *Inorg. Chim. Acta* **1998**, *274*, 7–14; e) J. Zank, A. Schier, H. Schmidbaur, *J. Chem. Soc., Dalton Trans.* **1999**, 415–420; f) F. I. Adam, G. Hogarth, I. Richards, B. E. Sanchez, *Dalton Trans.* **2007**, 2495–2498.
- [11] a) Z. Pan, M. T. Gamer, P. W. Roesky, *Z. Anorg. Allg. Chem.* **2006**, *632*, 743–748; b) J. I. van der Vlugt, E. A. Pidko, R. C. Bauer, Y. Gloaguen, M. K. Rong, M. Lutz, *Chem. Eur. J.* **2011**, *17*, 3850–3854; c) J. C. DeMott, F. Basuli, U. J. Kilgore, B. M. Foxman, J. C. Huffman, O. V. Ozerov, D. J. Mendiola, *Inorg. Chem.* **2007**, *46*, 6271–6276; d) F. Wei, X. Liu, Z. Liu, Z. Bian, Y. Zhao, C. Huang, *CrystEngComm* **2014**, *16*, 5338–5344; e) P. Arce, C. Vera, D. Escudero, J. Guerrero, A. Lappin, A. Oliver, D. H. Jara, G. Ferraudi, L. Lemus, *Dalton Trans.* **2017**, *46*, 13432–13445.
- [12] a) C. M. Frech, L. J. W. Shimon, D. Milstein, *Angew. Chem. Int. Ed.* **2005**, *44*, 1709–1711; b) T. Cheisson, A. Auffrant, *Dalton Trans.* **2014**, *43*, 13399–13409; c) X.-P. Zhang, V. Y. Chang, J. Liu, X.-L. Yang, W. Huang, Y. Li, C.-H. Li, G. Muller, X.-Z. You, *Inorg. Chem.* **2015**, *54*, 143–152; d) B. A. Schaefer, G. W. Margulieux, B. L. Small, P. J. Chirik, *Organometallics* **2015**, *34*, 1307–1320; e) D. Domyati, S. L. Hope, R. Latifi, M. D. Hearn, L. Tahsini, *Inorg. Chem.* **2016**, *55*, 11685–11693; f) S. C. Serin, F. S. Pick, G. R. Dake, D. P. Gates, *Inorg. Chem.* **2016**, *55*, 6670–6678.
- [13] a) P. Seviliano, A. Habtemariam, S. Parsons, A. Castineiras, M. E. Garcia, P. J. Sadler, *J. Chem. Soc., Dalton Trans.* **1999**, 2861–2870; b) M. P. Coogan, V. Fernandez-Moreira, B. M. Kariuki, S. J. A. Popoe, F. L. Thorp-Greenwood, *Angew. Chem. Int. Ed.* **2009**, *48*, 4965–4968; c) F. Raoof, A. R. Esmailbeig, S. M. Nabavizadeh, F. N. Hosseini, M. Kubicki, *Organometallics* **2013**, *32*, 3850–3858; d) S. Yu, Y. Dudkina, H. Wang, K. V. Kholin, M. K. Kadirov, Y. H. Budnikova, D. A. Vici, *Dalton Trans.* **2015**, *44*, 19443–19446.
- [14] B. R. M. Lake, C. E. Willans, *Chem. Eur. J.* **2013**, *19*, 16780–16790.
- [15] Selected examples: a) W. Schuh, H. Kopacka, K. Wurst, P. Peringer, *Chem. Commun.* **2001**, 2186–2187; b) M. Bardaji, A. Laguna, J. Vicente, P. G. Jones, *Inorg. Chem.* **2001**, *40*, 2675–2681; c) C. K.-L. Li, R. W.-Y. Sun, S. C.-F. Kui, N. Zhu, C.-M. Che, *Chem. Eur. J.* **2006**, *12*, 5253–5266; d) I. S. Krychankou, D. V. Krupenya, A. J. Karttunen, S. P. Tunik, T. A. Pakkanen, P.-T. Chou, I. O. Koshevoy, *Dalton Trans.* **2014**, *43*, 3383–3394; e) I. Marcos, V. Ojea, D. Vazquez-García, J. J. Fernández, A. Fernández, M. Lopez-Torres, J. Lado, J. M. Vila, *Dalton Trans.* **2017**, *46*, 16845–16860; f) D. T. Walters, R. B. Aghakhanpour, X. B. Powers, K. B. Ghiassi, M. M. Olmstead, A. L. Balch, *J. Am. Chem. Soc.* **2018**, *140*, 7533–7542.
- [16] a) P. L. Chiu, H. M. Lee, *Organometallics* **2005**, *24*, 1692–1702; b) S. Bestgen, M. T. Gamer, S. Lebedkin, M. M. Kappes, P. W. Roesky, *Chem. Eur. J.* **2015**, *21*, 601–614.
- [17] a) C. E. Strasser, V. J. Catalano, *J. Am. Chem. Soc.* **2010**, *132*, 10009–10011; b) C. E. Strasser, V. J. Catalano, *Inorg. Chem.* **2011**, *50*, 11228–11234; c) K. Chen, M. M. Nenzel, T. M. Brown, V. J. Catalano, *Inorg. Chem.* **2015**, *54*, 6900–6909.
- [18] D. A. Valyaev, J. Willot, L. P. Mangin, D. Zargarian, N. Lugan, *Dalton Trans.* **2017**, *46*, 10193–10196.
- [19] a) A. Hayashi, M. Okazaki, F. Ozawa, R. Tanaka, *Organometallics* **2007**, *26*, 5246–5249; b) J. I. van der Vlugt, E. A. Pidko, D. Vogt, M. Lutz, A. L. Spek, A. Meetsma, *Inorg. Chem.* **2008**, *47*, 4442–4444; c) C. Müller, E. A. Pidko, M. Lutz, A. L. Spek, D. Vogt, *Chem. Eur. J.* **2008**, *14*, 8803–8803; d) J. I. van der Vlugt, E. A. Pidko, D. Vogt, M. Lutz, A. L. Spek, *Inorg. Chem.* **2009**, *48*, 7513–7515; e) Y. Nakajima, Y. Shiraishi, T. Tsuchimoto, F. Ozawa, *Chem. Commun.* **2011**, 47, 6332–6334.
- [20] C.-M. Che, S.-W. Lai, *Coord. Chem. Rev.* **2005**, *249*, 1296–1309.
- [21] E. Kühnel, I. V. Shishkov, F. Rominger, T. Oeser, P. Hofmann, *Organometallics* **2012**, *31*, 8000–8011.
- [22] X. Han, L. L. Koh, Z.-P. Liu, Z. Weng, T. S. A. Hor, *Organometallics* **2010**, *29*, 2403–2405.
- [23] a) A. A. D. Tulloch, A. A. Danopoulos, S. Kleinhenz, M. E. Light, M. B. Hursthouse, G. Eastham, *Organometallics* **2001**, *20*, 2027–2031; b) C. Deißler, F. Rominger, D. Kunz, *Dalton Trans.* **2009**, *35*, 7152–7167; c) G. Venkatachalam, M. Heckenroth, A. Neels, M. Albrecht, *Helv. Chim. Acta* **2009**, *92*, 1034–1045; d) M. R. L. Furst, C. S. J. Cazin, *Chem. Commun.* **2010**, *46*, 6924–6925.
- [24] a) J. Zheng, S. Elongovan, D. A. Valyaev, R. Brousses, V. César, J.-B. Sortais, C. Darcel, N. Lugan, G. Lavigne, *Adv. Synth. Catal.* **2014**, *356*, 1093–1097; b) D. A. Valyaev, D. Wei, S. Elangovan, M. Cavailles, V. Dorcet, J.-B. Sortais, C. Darcel, N. Lugan, *Organometallics* **2016**, *35*, 4090–4098; c) R. Buhaibeh, O. A. Filippov, A. Bruneau-Voisine, J. Willot, C. Duhayon, D. A. Valyaev, N. Lugan, Y. Canac, J.-B. Sortais, *Angew. Chem. Int. Ed.* **2019**, *58*, 6727–6731.
- [25] D. H. Nguyen, X. Trivelli, F. Capet, J.-F. Paul, F. Dumeignil, R. M. Gauvin, *ACS Catal.* **2017**, *7*, 2022–2032.
- [26] a) P. P. Samuel, K. C. Mondal, H. W. Roesky, M. Hermann, G. Frenking, S. Demeshko, F. Meyer, A. C. Stückl, J. H. Christian, N. S. Dalal, L. Ungur, L. F. Chibotaru, K. Pröpper, A. Meents, B. Dittrich, *Angew. Chem. Int. Ed.* **2013**, *52*, 11817–11821; b) R. Fraser, C. G. C. E. van Sittert, P. H. van Rooyen, M. Landman, *J. Organomet. Chem.* **2017**, *835*, 60–69; c) J. Cheng, Q. Chen, X. Leng, Z. Ouyang, Z. Wang, S. Ye, L. Deng, *Chem* **2018**, *4*, 2844–2860; d) M. F. Pinto, M. Olivares, Á. Vivancos, G. Guisado-Barrios, M. Albrecht, B. Royo, *Catal. Sci. Technol.* **2019**, *9*, 2421–2425.
- [27] L. J. Farrugia, P. R. Mallinson, B. Stewart, *Acta Crystallogr. B* **2003**, *59*, 234–247.

-
- [28] B. Berzina, I. Sokolovs, E. Suna, *ACS Catal.* **2015**, *5*, 7008–7014.
- [29] L. J. Farrugia, *J. Appl. Crystallogr.* **2012**, *45*, 849–854.
- [30] A. Altomare, G. Cascarano, C. Giacovazzo, A. Guagliardi, *J. Appl. Crystallogr.* **1994**, *27*, 435–436.
- [31] G. M. Sheldrick, *Acta Crystallogr.* **2015**, *A71*, 3–8.
- [32] P. v. d. Sluis, A. L. Spek, *Acta Crystallogr.* **1990**, *A46*, 194–201.
-
